

Balmer lines of the symbiotic binary Z Andromedae during its 2006 outburst*

Nikolai A. Tomov¹, Mima T. Tomova¹, Dmitry V. Bisikalo²

¹ Institute of Astronomy and NAO, Bulgarian Academy of Science, BG-1784 Sofia

² Institute of Astronomy, Russian Academy of Science, RU-119017 Moscow
tomov@astro.bas.bg

(Accepted on 22.09.2011)

Abstract. High-resolution observations in the region of the Balmer H α and H γ lines of the spectrum of the symbiotic binary Z And were performed during its major eruption in 2006. The H α line had additional satellite high-velocity components situated on either side of its central peak which indicated bipolar collimated outflow from the compact object. The H γ line presented three components, consisting of a central narrow emission, a broad emission component with low intensity indicating an optically thin stellar wind with a velocity of about 500 km s⁻¹ from the compact object and a blueshifted P Cyg absorption with a multi-component structure occupying a broad velocity range. These data are explained in the light of a model where a disc-like envelope surrounding the accretion disc collimates the stellar wind of the compact object and gives rise to bipolar outflow. The mass-loss rate of the accretor was derived at several epochs after the light maximum. We conclude that the mass-loss rate has decreased probably from $4-5 \times 10^{-7} (d/1.12\text{kpc})^{3/2} M_{\odot} \text{yr}^{-1}$ at the time of maximum light to about $2 \times 10^{-7} (d/1.12\text{kpc})^{3/2} M_{\odot} \text{yr}^{-1}$ in 2006 December.

Key words: binaries: symbiotic - stars: activity - stars: mass-loss - stars: winds, outflows - stars: individual: Z And

Балмерови линии на симбиотичната двойна система Z Andromedae по време на избухването ѝ през 2006 г.

Николай А. Томов, Мима Т. Томова и Дмитрий В. Бисикало

Проведени са наблюдения в областите на Балмеровите линии H α и H γ от спектъра на симбиотичната двойна звезда Z And по време на голямото ѝ избухване през 2006 г. Линията H α имаше допълнителни високоскоростни компоненти, разположени от двете страни на централната емисия, които показваха биполярно колимирано изтичане от компактния обект. Линията H γ имаше три компонента – централна тясна емисия, широк емисионен компонент с ниска интензивност, индикиращ оптически тънък звезден вятър със скорост около 500 km s⁻¹ от компактния обект и синьо отместена многокомпонентна P Cyg абсорбция, заемаща широк интервал по лъчеви скорости. Тези данни са обяснени в светлината на модел, в който дископодобна обвивка около акреционния диск колимира звездния вятър от компактния обект и формира биполярно изтичане. Получен е темпът на загуба на маса от акретора в различни моменти след максимума на блясъка. Ние стигнахме до извода, че темпът на загуба на маса вероятно е намалял от $4-5 \times 10^{-7} (d/1.12\text{kpc})^{3/2} M_{\odot} \text{yr}^{-1}$ във времето на максимума на блясъка до около $2 \times 10^{-7} (d/1.12\text{kpc})^{3/2} M_{\odot} \text{yr}^{-1}$ през декември 2006 г.

Introduction

Symbiotic stars are long-period interacting binaries consisting of a cool visual primary and a hot compact secondary component accreting matter from the

* Based on observations collected at the Rozhen National Astronomical Observatory, Bulgaria

atmosphere of its companion. The nature of collimated jets from symbiotic stars is the subject of intensive theoretical investigation and the view that they represent outflow from an accreting compact object is widely accepted (Zanni et al. 2007). The collimated bipolar outflow, however, could arise due to a stellar wind, if the mechanism of collimation is available in the system. Such a mechanism can be related to disc-like formation surrounding the white dwarf which provides a small opening angle of the outflowing jets.

The system Z And is considered as a prototype of the classical symbiotic stars. Its last active phase began at the end of 2000 August (Skopal et al. 2000) and continues up to now including six (or seven?) optical eruptions. During the historical 2006 eruption optical collimated bipolar outflow was well observed along with other mass-loss mechanisms (Burmeister & Leedjarv 2007, Tomov et al. 2007, Skopal et al. 2009, Tomov et al. 2010).

According to the modern theory, the existence of bipolar collimated jets is supposed to be due to the presence of a magnetic disc which transforms the potential energy of the accreting material into kinetic energy of the outflowing gas. This means that the accreting material provides the jet outflow. However, different indications of stellar wind were present along with satellite emission components implying a collimated bipolar outflow in the spectrum of Z And during its 2006 outburst. Therefore, accretion and stellar wind from the compact object must happen at the same time. To avoid this difficulty we propose another model for the interpretation of the spectrum, namely one with collimated stellar wind.

A model of collimated stellar wind was suggested in the works of Tomov et al. (2010, 2011) to explain the basic spectral features of Z And during its 2000, 2002 and 2006 eruptions. The main aim of our present work is to propose an explanation for the $H\alpha$ and $H\gamma$ lines during the major 2006 eruption of Z And in the framework of this model.

1 Observations and reduction

The regions of the $H\alpha$ and $H\gamma$ lines of the spectrum of Z And were observed on fourteen nights during 2006 July – December covering its major eruption with the Photometrics CCD camera mounted on the Coude spectrograph of the 2m Ritchey-Chretien-Coude (RCC) telescope of the National Astronomical Observatory Rozhen. The spectral resolution was 0.2 Å/px on all occasions. When more than one exposure was taken per night, the spectra were added with the aim of improving the signal-to-noise ratio. The IRAF package³ was used for the data reduction as well as for obtaining the dispersion curve, calculating the radial velocities and equivalent widths.

The absolute fluxes of the $H\alpha$ and $H\gamma$ lines were calculated by using their equivalent widths and the continuum fluxes at their positions. The continuum flux at the position of the $H\gamma$ line was obtained using linear extrapolation of the B and V photometric fluxes taken on the same, or close, nights from the paper of Skopal et al. (2007). To obtain the $H\alpha$ flux we used the Cousins R_c

³ The IRAF package is distributed by the National Optical Astronomy Observatories, which is operated by the Association of Universities for Research in Astronomy, Inc., under contract with the National Science Foundation.

photometric band flux from the same paper supposing that it is practically equal to the continuum flux at the position of $H\alpha$. The BV fluxes were not corrected for the intensive emission lines of Z And because of the strong increase of the stellar and nebular continua and the relative decrease of the emission lines. The uncertainty of the continuum flux is not more than 10 per cent. All the fluxes were also corrected for the interstellar reddening of $E(B - V) = 0.30$ using the extinction law of Cardelli et al. (1989).

We assumed $\text{Min}(\text{vis}) = \text{JD } 2\,442\,666^{\text{d}}.0 + 758^{\text{d}}.8 \times E$ (Tomov et al. 2010, 2011), where the orbital period is calculated from both photometric and spectral data, and the epoch of the orbital photometric minimum coincides with that of the spectral conjunction (Formigini & Leibowitz 1994, Mikolajewska & Kenyon 1996, Fekel et al. 2000).

2 Analysis of the Balmer lines

2.1 $H\alpha$ line

The first eight of our spectra taken around the $H\alpha$ line were considered in the work of Tomov et al. (2007). According to these data the line consisted of strong central narrow emission component (core), located around the reference wavelength, a broad emission component with low intensity (wings) and additional absorption and emission features on both sides of the central component (Fig. 1). The central component presented shoulder(s) on its short-wavelength side, which was not visible on the spectra taken in September. A weak peak component on the short-wavelength side of the central component is seen in the spectrum of August 8 and the dip feature between them indicates a moderate velocity of about 100 km s^{-1} . The other spectra (Fig. 1) show that at the rest of the time of our observations the line consisted of the same components. Very weak peak component on the short-wavelength side of the central component was seen again from October 31. The high-velocity satellite emission components were approximated with a Gaussian and the other part of the line (the core together with the wings) – with two or three Lorentzians. The uncertainty of the equivalent width of the satellite emissions was not more than 30 per cent and that of the whole line – about 2 per cent.

High resolution $H\alpha$ data taken in quiescent before the 2000 – 2011 active phase were analysed in the work of Tomov et al. (2008) and it was concluded that the broad wings of the line extending to velocities not smaller than about 2000 km s^{-1} from its centre are formed mainly through Raman scattering of $\text{Ly}\beta$ photons by atomic hydrogen in the wind of the giant. It was also concluded that radiation damping has probably some contribution in these wings too. On 2006 July the red wing of the broad component was appreciably more intensive than the blue one. Skopal (2006) suggested that the $H\alpha$ wings of the symbiotic stars during their active phases form in the high velocity wind of their compact component. Based on this suggestion Skopal et al. (2009) concluded that the $H\alpha$ wings of Z And during the 2006 brightening are also determined from stellar wind. However, attention should be paid to the fact that the FWZI of the $H\alpha$ wings of Z And was the same in both

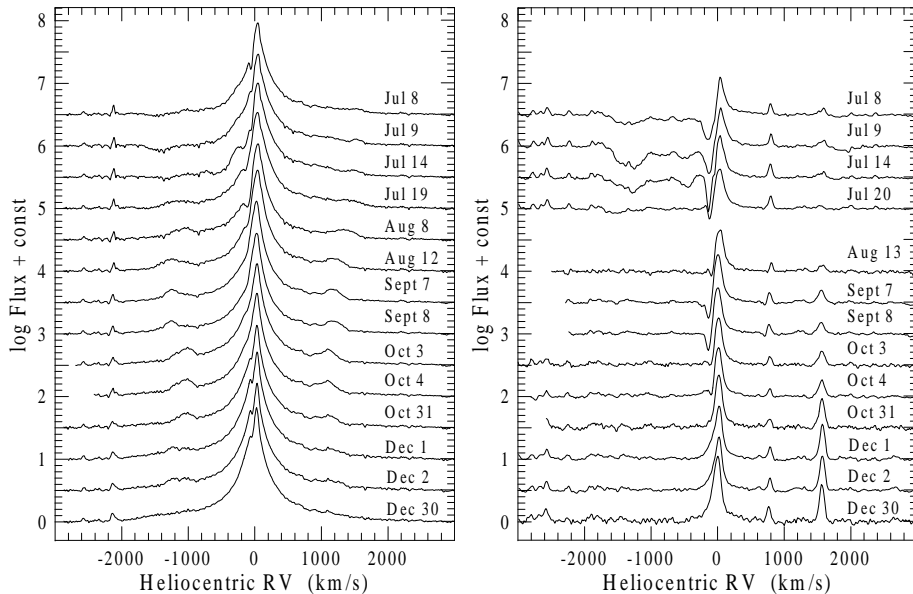


Fig. 1. Time evolution of the H α (left panel) and H γ (right panel) lines.

stages of the system, the quiescent and active ones, maintaining its value of about 4000 km s^{-1} . This fact gives us some reason to suppose that during the 2006 brightening the FWZI of the wings was determined mainly from radiation damping like in the quiescent state of the system and the stellar wind emitted at smaller distance from the centre of the line. The problem on the nature of the H α wings needs to be considered further.

Together with the central narrow and broad components the H α line presented additional satellite components with velocity of more than 1000 km s^{-1} situated on either side of the central component (Fig. 1). The view that they are an indication of bipolar collimated outflow from the compact object is commonly accepted (Burmeister & Leedj arv 2007, Tomov et al. 2007, Skopal et al. 2009). We associated these components with collimated stellar wind. They can be interpreted in the light of a model suggested earlier by us and acceptable if the inclination angle does not exceed 55° (Tomov et al. 2010, 2011).

The first of our spectra, taken in July, show one pronounced absorption with a velocity of 1400 km s^{-1} on the short-wavelength side of the central component of the line and only weak emission component, irregularly shaped and having velocity of about 1500 km s^{-1} on its long-wavelength side. The absorption indicates mass outflow which projects on to the observed photosphere of the outbursting compact object (its disc-like shell). As is seen from the evolution of the spectrum the absorption component disappears and emission appears. Thus two emission components on the two sides of the

Table 1. The H α line data. $F(t)$ is the total H α flux and \dot{M}_{cw} is sum of the mass-loss rates based on the satellite line components. All fluxes are in units of 10^{-12} erg cm $^{-2}$ s $^{-1}$, the mass-loss rates – in units of $10^{-7}(\text{d}/1.12\text{kpc})^{3/2} \mathcal{M}_{\odot} \text{yr}^{-1}$ and the radial velocities – in units of km s $^{-1}$.

Date	$F(t)$	Blue			Red			M_{cw}
		RV	F	\dot{M}	RV	F	\dot{M}	
Jul 19	332.527	−1196	1.675	1.03	1445	1.675	0.85	1.88
Aug 8	279.490	−1087	2.883	1.17	1346	3.244	1.27	2.44
Aug 12		−1260	4.407	1.54	1201	3.526	1.03	2.57
Sept 7	262.478	−1245	2.642	0.50	1178	2.936	0.61	1.11
Sept 8	257.047	−1262	2.496	0.42	1196	3.083	0.78	1.20
Oct 3	264.773	−1050	4.071	1.27	1112	3.053	0.54	1.81
Oct 4	270.444	−1070	4.071	1.15	1099	3.053	0.61	1.76
Oct 31	241.650	−1054	2.295	0.60	1132	1.620	0.38	0.98
Dec 1	251.334	−1214	1.577	0.75	1174	1.092	0.54	1.29
Dec 2	250.484				1185	1.092	0.70	>0.70
Dec 30	279.816							

central peak form after the middle of July and were visible until December. The disappearance of the blueshifted absorption component and the development of emission are most probably due to a decrease of the mass-loss rate of the compact object and/or increase of the number of emitting atoms in that area of the wind which does not project on to the observed photosphere. The evolution of the spectrum (Fig. 1, Table 1) shows also that the line flux of the satellite components after the beginning of October decreases with time, which is due to decrease of the mass-loss rate of the compact object too.

2.2 H γ line

During the 2006 brightening the H γ line presented a broad emission component with low intensity and FWZI of about 1000 km s $^{-1}$ in addition to its central narrow component with a nebular profile. The broad component is best seen on the spectra taken after 2006 October 31 (Figs. 1 and 2). The data obtained in this period of time show that the energy flux of the broad component decreased when the light weakened after its maximum, whereas the behaviour of the central narrow emission was different (Table 2). The broad component was analysed by approximating with a Gaussian function (Fig. 2, left panel), and its parameters obtained with this procedure are listed in Table 2. The error of the equivalent width due to the uncertainty of the continuum level reaches up to 10 per cent. On the spectra taken in July – September the blue wing of the broad component was not seen because of blending with the P Cyg absorption component (see below and Fig. 1, left panel). On the spectra taken in October and December the blue wing appeared to be less extended than the red one due to blending with the P Cyg absorption. We consider that the broad emission component indicates an optically thin stellar wind with a high velocity of about 500 km s $^{-1}$ from the compact object in the system.

On the spectra taken during 2006 July – September the central narrow component of the line had positive radial velocity, which was due to presence

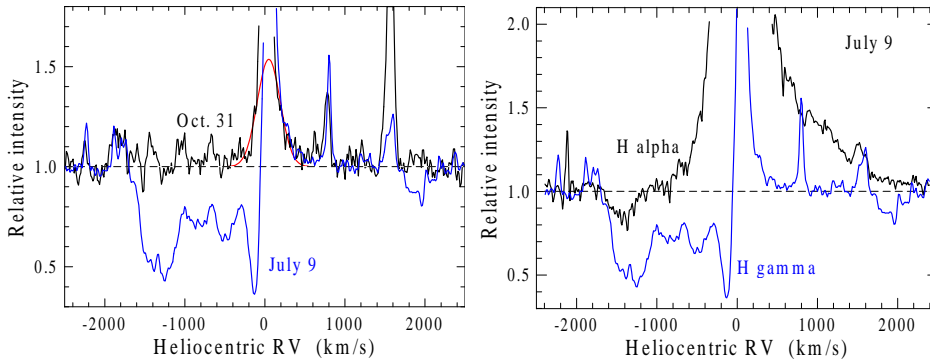


Fig. 2. Left panel: The profile of the $H\gamma$ line on July 9 and October 31. The Gaussian fit of the broad component is also shown. The level of the local continuum is marked with a dashed line. Right panel: The profile of the $H\alpha$ and $H\gamma$ lines on July 9. The level of the local continuum is marked with a dashed line.

Table 2. The $H\gamma$ line data. N denotes narrow component and B – broad component. F is in units 10^{-12} erg cm^{-2} s^{-1} , \dot{M} and \dot{M}_w are in units $10^{-7}(\text{d}/1.12 \text{ kpc})^{3/2} \mathcal{M}_\odot \text{yr}^{-1}$ and $\dot{M} = \dot{M}_w + \dot{M}_{\text{cw}}$.

Date	FWHM(N) (km s^{-1})	F (N)	FWHM(B) (km s^{-1})	FWZI(B) (km s^{-1})	v_w (km s^{-1})	F (B)	\dot{M}_w	\dot{M}
Oct 31	85.6	20.174	340 ± 40	746	370	7.834	1.05	2.03
Dec 1	82.9	20.003	430 ± 40	981	490	6.209	1.14	2.43
Dec 2	82.9	20.074	480 ± 50	1022	510	6.280	1.20	>1.90

of a blueshifted P Cyg absorption (Figs. 1 and 2). In July this absorption presented multi-component structure and occupied a velocity range from about 100 to 1500–1600 km s^{-1} . After that it gradually weakened and converted in low velocity absorption presenting in the spectrum until the beginning of 2006 October (Fig. 1). The residual intensity of this absorption was minimal in the middle of July at 0.4. As the cool giant’s continuum, at the same time, was less than 9 per cent of the total continuum of the system at the wavelength position of the B photometric band (Skopal et al. 2009) which is close to the $H\gamma$ line, the P Cyg absorption may be related to the optically thick mass outflow from the outbursting compact object. The comparison of the spectra taken on July 9 and October 31 shows that the red wing of the broad component on the two spectra coincide (Fig. 2), which suggests that the $H\gamma$ line has also three components, consisting of a central narrow emission component, a broad emission component with low intensity and multi-component P Cyg absorption occupying broad region of velocities of the outflowing material – from about 100 to 1500–1600 km s^{-1} .

In the framework of our model (Tomov et al. 2010, 2011) the three-component line can be interpreted in the following way. The high velocity wind indicated by the broad emission component collides with the disc and

disc-like envelope and after the collision the outflowing material moves close to the surface of the cone. This part of the material which is between the observed photosphere of the outbursting compact object (the disc-like shell) and the observer gives rise to the P Cyg absorption.

The position of the most blueshifted component of the $H\gamma$ absorption was very close to the position of the $H\alpha$ absorption, which suggests the $H\gamma$ component arises in the same velocity region. The $H\gamma$ absorption however, presented additional components with lower velocities which arise probably closer to the compact object (Fig. 2).

3 Mass-loss rate

According to the model we suggested the wind of the outbursting compact object associated with the broad emission component of the $H\gamma$ line is collimated by the disc-like envelope and the collimated outflow is observed as the satellite emission components of the $H\alpha$ line. These two lines appear in different regions of the outflow but both of them indicate mass-loss. The total mass-loss rate of the compact object is obtained as a sum of the mass-loss rates, based on each of these lines. The mass-loss rate was determined from the energy flux of the lines supposing that the outflow was constant using the nebular approach (Vogel & Nüssbaumer 1994).

The mass-loss rate based on the broad $H\gamma$ emission component was calculated from the spectra obtained from October 31, since the period prior to it the blue wing of the $H\gamma$ line was absorbed by the wind outflow responsible for the P Cyg absorption (Table 2). On the spectra used the broad $H\gamma$ component was not symmetric as its blue wing was partly absorbed by the P Cyg type wind outflow with low velocity. Having in mind this absorption we consider the $H\gamma$ wind velocity and the corresponding mass-loss rate as a lower limit.

The particle density in the wind is expressed via the continuity equation. In our calculations, we adopted a value of the electron temperature in the wind of 30 000 K like during the first outburst (Tomov et al. 2008). We used a parameter $\mu = 1.4$ (Nüssbaumer & Vogel 1987), determining the mean molecular weight μm_H in the wind and a helium abundance of 0.1 (Vogel & Nüssbaumer 1994). We adopted a distance to the system $d=1.12$ kpc (Fernandez-Castro et al. 1988, 1995) to compare the results with our previous paper on Z And more easily. It is supposed that the line is emitted by a spherical layer and the radii of integration must be estimated. We assumed optically thin medium and the inner radius in this case is thought to be the photospheric radius. The photospheric radius was estimated from the bolometric luminosity and the effective temperature of the outbursting compact object at the time of each observation. We used a bolometric luminosity of $10^4 \mathcal{L}_\odot$ (Sokoloski et al. 2006) and Zanstra temperature from Burmeister & Leedj arv (2007) and Burmeister (2010). The outer radius of integration was $14 \mathcal{R}_\odot$ (see below). We used a recombination coefficient for case B (Storey & Hummer 1995) corresponding to temperature of 30 000 K and the density at the level of the photosphere at the time of each observation. The results are presented in Table 2.

The mass-loss rate based on the $H\alpha$ satellite emission components was calculated for each observation. The wind outflow was considered to occupy a spherical sector with opening angle θ and solid angle Ω . These angles were calculated using the approach of Skopal et al. (2009). With an upper limit of the inclination angle of the system of 55° we obtained average values of the lower limit of the opening angle of the spherical sector of $\theta(f) = 18.4^\circ \pm 1.1^\circ$ for the front wind component and $\theta(b) = 16.8^\circ \pm 0.7^\circ$ for the back wind component.

The next step is to estimate the radii of integration. The broad component of the $H\gamma$ line and the satellite $H\alpha$ components are emitted in regions with different velocity fields. We assume that the satellite $H\alpha$ components are emitted in the region of the wind where the velocity is at a maximum. The inner radius of this region was determined in the next way. The absorption satellite component is an indication of mass outflow which is projected on to the observed photosphere of the outbursting compact object (its disk-like shell). The radius of this photosphere according to Skopal et al. (2009) is $12 \pm 4 \mathcal{R}_\odot$ at a distance to the system of 1.5 kpc. Baring in mind the error on the observation, a radius of $10 \mathcal{R}_\odot$ at a distance of 1.12 kpc is acceptable. Assuming a diameter of the disc-like shell of $20 \mathcal{R}_\odot$ and the inclination angle of 55° for the inner radius of the region of the collimated wind we obtain $14 \mathcal{R}_\odot$. We adopted an outer radius of the region of the collimated wind of infinity. We used a recombination coefficient for case B (Storey & Hummer 1995) corresponding to a temperature of 30 000 K and density at distance of $14 \mathcal{R}_\odot$ from the compact object at the time of each observation. The results are presented in Table 1.

The total mass-loss rate, which is the sum of the mass-loss rates based on the two lines, is listed in the Table 2. The data in the Table 1 show that the mass-loss rate based on the satellite $H\alpha$ components decreases with the optical light of the system. It is about $2 \times 10^{-7} (d/1.12\text{kpc})^{3/2} \mathcal{M}_\odot \text{yr}^{-1}$ at the time of the light maximum and decreases to about $1 \times 10^{-7} (d/1.12\text{kpc})^{3/2} \mathcal{M}_\odot \text{yr}^{-1}$ in 2006 December. The mass-loss rate based on the $H\gamma$ data from October and December is equal to the $H\alpha$ rate at those time. This result proposes that the rate based on $H\gamma$ probably has been close to that of $H\alpha$ at the time of the maximum light and has been decreasing at the same rate. Therefore, we can conclude the total mass-loss rate of the compact object has been $4\text{--}5 \times 10^{-7} (d/1.12\text{kpc})^{3/2} \mathcal{M}_\odot \text{yr}^{-1}$ at the time of maximum light and has decreased to about $2 \times 10^{-7} (d/1.12\text{kpc})^{3/2} \mathcal{M}_\odot \text{yr}^{-1}$ in 2006 December.

4 Discussion

The data in the Tables 1 and 2 show the energy flux of the $H\alpha$ satellite components decreases when the flux of the $H\gamma$ broad component also decreases, which imply that the collimated outflow emitted most of its material when the wind was strongest. Tight correlation between the strength of the $H\alpha$ satellite components and the HeI P Cyg absorption indicating stellar wind from the compact object in the system Hen 3-1341 was found by Munari et

al. (2005) during the phase of activity between 1989 and 2004 of this system. The authors wrote "The jets were most prominent when the wind was strongest, and declined in parallel with the decrease of wind intensity.". They came to the conclusion that the wind plays a role of feeding mechanism for the collimated outflow. The spectral behaviour of Hen 3-1341 during its active phase was identical to that of Z And. In light of our model of Z And the wind plays a role of feeding mechanism for the collimated outflow too.

5 Conclusions

We present the results of high-resolution observations of the H α and H γ lines of the symbiotic prototype Z And carried out during 2006 light maximum and after it. The profile of the H α line was a multi-component one consisting of an intense central narrow emission located around the reference wavelength, a broad emission component with low intensity (wings) and additional high-velocity absorption and emission features on both sides of the central emission indicating bipolar collimated outflow from the compact object in the system.

The profile of H γ was three-component, consisting of central narrow emission, a broad emission component with low intensity and a blueshifted absorption of the type P Cyg. The broad emission component was present in the spectrum during the whole time of our observations – from July until December 2006. In July the P Cyg absorption had multi-component structure being situated in a broad velocity range from about 100 km s⁻¹ to 1500–1600 km s⁻¹. After that it gradually weakened towards low velocity absorption seen in the spectrum until the beginning of October 2006. In July the velocity position of the most blueshifted component of the H γ absorption was very close to the position of the H α absorption.

The behaviour of the lines is considered in the framework of model suggested for interpretation of the line spectrum of Z And during the 2000 – 2011 active phase. It is supposed that the high-velocity wind from the compact object observed in the broad emission component of the line H γ collides with the accretion disc and the disc-like envelope which plays the role of mechanism of collimation. After the collision the wind is collimated and is observed in both groups of lines, the high-velocity satellite H α components and the H γ P Cyg absorption.

The mass-loss rate of the compact object was estimated at several epochs of the eruption. The rate was found to decrease, from $4\text{--}5 \times 10^{-7} \text{ (d/1.12kpc)}^{3/2} \mathcal{M}_{\odot} \text{ yr}^{-1}$ at the time of maximum light to about $2 \times 10^{-7} \text{ (d/1.12kpc)}^{3/2} \mathcal{M}_{\odot} \text{ yr}^{-1}$ in 2006 December.

Acknowledgments

This work has been supported by the Bulgarian Scientific Research Fund (Grant DO 02-85), the Basic Research Program of the Presidium of the Russian Academy of Sciences, Russian Foundation for Basic Research (projects 11-02-00076, 11-02-01248), Federal Targeted Program "Science and Science

Education for Innovation in Russia 2009-2013“ and the Russian and Bulgarian Academies of Sciences through a collaborative program in basic space research.

References

- Burmeister M., 2010, Ph.D. Thesis, Tartu University Press, Tartu, p.35
 Burmeister M. & Leedjarv L., 2007, *A&A*, 461, 5L
 Cardelli J. A., Clayton G. C., Mathis J. S., 1989, *ApJ*, 345, 245
 Fekel F. C., Hinkle K. H., Joyce R. R., Skrutskie M. F., 2000, *AJ*, 120, 3255
 Fernandez-Castro T., Cassatella A., Gimenez A., Viotti R., 1988, *ApJ*, 324, 1016
 Fernandez-Castro T., Gonzalez-Riestra R., Cassatella A., Taylor A., Seaquist E.R., 1995, *ApJ*, 442, 366
 Formigini L. & Leibowitz E. M., 1994, *A&A*, 292, 534
 Mikolajewska J. & Kenyon S. J., 1996, *AJ*, 112, 1659
 Munari U., Siviero A., Henden A., 2005, *MNRAS*, 360, 1257
 Nüssbaumer H. & Vogel M., 1987, *A&A*, 182, 51
 Skopal A. 2003, *A&A*, 401, 17L
 Skopal A. 2006, *A&A*, 457, 1003
 Skopal A., Chochol D., Pribulla T., Vanko M., 2000, *IBVS*, 5005
 Skopal A., Pribulla T., Budaj J. et al., 2009, *ApJ*, 690, 1222
 Skopal A., Vaňko M., Pribulla T., Chochol D., Semkov E., Wolf M., Jones, A. 2007, *AN*, 328, 909
 Sokoloski J.L. et al., 2006, *ApJ*, 636, 1002
 Storey P. J. & Hummer D. G. 1995, *MNRAS*, 272, 41
 Tomov N. A., Bisikalo D. V., Tomova M. T., Kilpio E. Yu., 2011, in 3RD SCHOOL AND WORKSHOP ON SPACE PLASMA PHYSICS, eds. I. Zhelyazkov & T. Mishonov, AIP Conf. Proc., 1356, 35
 Tomov N. A., Taranova O. G., Tomova M. T., 2003, *A&A*, 401, 669
 Tomov N.A., Tomova M.T., Bisikalo D.V., 2007, *MNRAS*, 376, L16
 Tomov N.A., Tomova M.T., Bisikalo D.V., 2008, *MNRAS*, 389, 829
 Tomov N.A., Tomova M.T., Bisikalo D.V., Kilpio E. Yu., 2010, *Astronomy Reports*, 54, 628
 Vogel M., Nüssbaumer H., 1994, *A&A*, 284, 145
 Zanni C., Ferrari A., Rosner R., Bodo G., Massaglia S., 2007, *A&A*, 469, 811